Vascular Health and Risk Management

Dovepress
Taylor & Francis Group

Open Access Full Text Article

ORIGINAL RESEARCH

Distal Venous Arterialization Modulates Autophagy-Related Markers in Skeletal Muscle in a Rat Hindlimb Ischemia Model

Teguh Marfen Djajakusumah[1], Bethy Suryawathy Hernowo[2], Pei Ho[3], Herry Herman[4], Kiki Lukman[5], Ronny Lesmana[6]

[1]Division of Vascular and Endovascular Surgery, Department of Surgery, Universitas Padjadjaran – Hasan Sadikin Hospital, Bandung, Indonesia; [2]Department of Pathology, Universitas Padjadjaran – Hasan Sadikin Hospital, Bandung, Indonesia; [3]Department of Surgery, National University of Singapore, Singapore, Singapore; [4]Department of Orthopaedic Surgery, Universitas Padjadjaran – Hasan Sadikin Hospital, Bandung, Indonesia; [5]Department of Surgery, Universitas Padjadjaran – Hasan Sadikin Hospital, Bandung, Indonesia; [6]Department of Physiology, Universitas Padjadjaran, Bandung, Indonesia

Correspondence: Teguh Marfen Djajakusumah, Department of Vascular and Endovascular Surgery, Department of Surgery, Universitas Padjadjaran-Hasan Sadikin Hospital, Jl. Pasteur No. 38, Pasteur, Kec. Sukajadi, Bandung, Jawa Barat, 40161, Indonesia, Tel +628122023770, Email marfen.djajakusumah@unpad.ac.id

Background: Distal venous arterialization (DVA) is a surgical option for limb salvage in peripheral arterial disease (PAD) without distal runoff. While increasingly applied, the skeletal muscle response after arterial–venous anastomosis remains unclear. This study evaluated skeletal muscle adaptation following DVA, focusing on autophagy regulation.

Methods: This experimental preclinical study evaluated skeletal muscle adaptation following distal venous arterialization (DVA) in a rat hindlimb ischemia model. An experimental microsurgical study was conducted in 30 Wistar rats. Hindlimb ischemia (HLI) was induced by right femoral artery ligation. On day 7, rats were re-operated and divided into DVA, opened ligation (OL), or persistent ligation (HLI) groups, with contralateral limbs serving as sham. On day 14, skeletal muscles were harvested for capillary density (CD31) and Western blot analysis of HIF-1α, AMPK, LC3-II, and p62. Gait analysis (stride length and width) and limb thermography were also performed.

Results: At day 7, HLI showed significant stride length reduction (p=0.029) and lower limb temperature (p<0.001). By day 14, gait and thermography normalized in DVA and OL but remained impaired in HLI (p=0.041 and p<0.001, respectively). Capillary density increased in HLI compared with sham (p=0.031), but not in DVA or OL. HIF-1α and AMPK were elevated in HLI (p=0.016 and p=0.011), while AMPK decreased in DVA (p=0.044). LC3-II expression was reduced in DVA compared with sham and HLI (p=0.002 and p=0.032). No significant differences were observed in p62.

Conclusion: DVA enhances skeletal muscle recovery in ischemic limbs and is associated with normalization of hypoxia- and autophagy-related molecular markers.

Keywords: autophagy, physiological adaptation, distal venous arterialization, hindlimb ischemia, LC3-II

Introduction

Peripheral arterial disease (PAD) affects over 113 million people worldwide and is a major cause of disability and limb loss.[1] Also known as lower extremity arterial disease (LEAD), PAD is characterized by atherosclerotic narrowing or occlusion of lower extremity arteries, resulting in insufficient perfusion and progressive ischemia.[1–3] Clinical manifestations range from intermittent claudication to ischemic rest pain and gangrene.[4] Management depends on severity and includes lifestyle modification, pharmacotherapy, surgical bypass, or endovascular revascularization.[3] In patients without viable distal runoff, conventional revascularization is not feasible, and major amputation remains the only option—accounting for approximately 51–93% of all lower extremity amputations.[5] Distal venous arterialization (DVA) has emerged as an alternative revascularization strategy for such inoperable limbs.[6] By creating an arterial–venous anastomosis, DVA redirects blood flow into the venous system to reperfuse ischemic tissue. While clinical studies and meta-analyses have demonstrated promising outcomes,[7] the mechanisms by which DVA influences skeletal muscle physiology

https://doi.org/10.2147/VHRM.S572547
Received: 7 October 2025
Accepted: 3 March 2026
Published: 24 March 2026

remain poorly defined. Autophagy, a cellular process responsible for degrading and recycling damaged proteins and organelles, plays a critical role in skeletal muscle adaptation.[8,9] During hypoxia, autophagy is regulated by hypoxia-inducible factor 1-alpha (HIF-1α) and AMP-activated protein kinase (AMPK).[10–13] HIF-1α promotes autophagy through BNIP3-mediated pathways, while AMPK functions as an energy sensor that activates autophagy during metabolic stress.[14] Although autophagy is protective under moderate stress, excessive activation has detrimental effects, potentially leading to cell death.[8,12,13,15] To date, no experimental studies have specifically examined the effects of DVA on ischemic skeletal muscle and its regulation of autophagy.[7] We therefore hypothesized that DVA would improve skeletal muscle function in a rat hindlimb ischemia (HLI) model and would be associated with modulation of autophagy-related signaling. This study was conducted in accordance with the ARRIVE 2.0 guidelines. Although this femoral artery ligation model does not fully replicate the chronic, multifactorial progression of clinical chronic limb-threatening ischemia, it reliably produces sustained reductions in perfusion, functional impairment, and hypoxia-related molecular responses. Therefore, it serves as a controlled experimental platform to investigate mechanistic adaptations to ischemia and the physiological effects of revascularization strategies such as distal venous arterialization.

Materials and Methods

Animals

Thirty healthy male *Wistar rats* (*Rattus norvegicus*), aged 18–20 weeks and weighing 300–350 g, were obtained from PT. Bio Farma (LLC, Indonesia). All animals were housed under a 12-hour light/12-hour dark cycle at a controlled room temperature of 26–29 °C, with ad libitum access to drinking water and standard laboratory feed. A 4-week acclimatization period was conducted at the Animal Husbandry Laboratory, Universitas Padjadjaran.

Grouping

This was an experimental microsurgical study. On day 0, all rats underwent ligation of the right common femoral artery to establish a hindlimb ischemia (HLI) model. On day 7, animals were allocated into three groups: (1) the distal venous arterialization (DVA) group, (2) the opened ligation (OL) group, and (3) the persistent ligation (HLI) group serving as ischemic controls. All groups were terminated on day 14 for skeletal muscle sampling. Untreated contralateral (left) limbs were used as sham controls to minimize animal use.

Sample size was determined using the Federer formula, requiring a minimum of six animals per group plus 1–2 reserve animals. To reduce the risk of technical failure, the DVA group—considered the most challenging microsurgical procedure—included 15 animals, while the OL and HLI groups consisted of 8 and 7 animals, respectively.

Randomization

Randomization was performed prior to HLI induction using permuted blocks of unequal size. Block allocations followed a 15:8:7 ratio (DVA:OL:HLI), consisting of blocks of six (3 DVA, 2 OL, 1 HLI) and blocks of twelve (6 DVA, 2 OL, 4 HLI). Three blocks of six and one block of twelve were employed. Allocation concealment and blinding were implemented by laboratory staff independent of the surgical and assessment teams.

Exclusion Criteria and Disqualification

Animals showing signs of illness or gait abnormalities before treatment were excluded. Disqualification criteria included unintended injury, perioperative death, surgical wound infection, foot gangrene, or technical failure of DVA or OL procedures. DVA failure was defined as thrombus formation at the arterial–venous anastomosis site, while OL failure was defined as thrombosis in the previously ligated artery upon tissue harvesting. Only healthy animals meeting predefined inclusion criteria were enrolled in the study. Animals with signs of illness, injury, or abnormal baseline conditions were not included prior to randomization. No animals were excluded after study initiation or from the final analysis.

Surgical Technique

Preoperative Preparation

Prior to surgery, body weight was recorded, gait footprints were obtained for subsequent analysis,[16] and thermal images of both hindlimbs were taken. Preoperative fasting was not required. Anesthesia was induced with an intraperitoneal injection of ketamine (Ket-A-100®, 200mg/kg) and xylazine (Xyla®, 28mg/kg) prepared in a 1 mL syringe. Unconsciousness was achieved within approximately 5 minutes and lasted for ~45 minutes. Intubation, oxygen supplementation, and continuous monitoring were not required.

Hindlimb Ischemia (HLI) Model Creation

The groin and medial thigh were shaved, and the rat was fixed in a supine position on a wooden board covered with an underpad sheet. The skin was prepared with 70% alcohol and 10% povidone-iodine solution. The board was placed in a tray positioned under an electronic surgical microscope (Eakins® digital microscope). A 7.0× surgical loupe was also used to aid magnification.

A longitudinal incision was made in the medial thigh using a No. 11 scalpel blade. The common femoral artery (CFA) and its branches, the superficial femoral artery (SFA) and deep femoral artery (DFA), as well as the femoral vein (FV), were carefully dissected. The CFA was isolated from the FV and secured with 7–0 polypropylene sutures (Optilene®, C3090545). Small arterial branches were identified but not ligated. The CFA was then ligated with a reef knot using the same suture. The incision was closed with 4–0 absorbable monofilament glyconate sutures (Monosyn®). While still anesthetized, a second thermal image was obtained (Figure 1A–D). Postoperatively, oral paracetamol syrup (120 mg/5 mL; 0.1 mL = 4.5 mg, two drops by pipette) was administered. Rats were returned to warmed cages and monitored daily for complications.

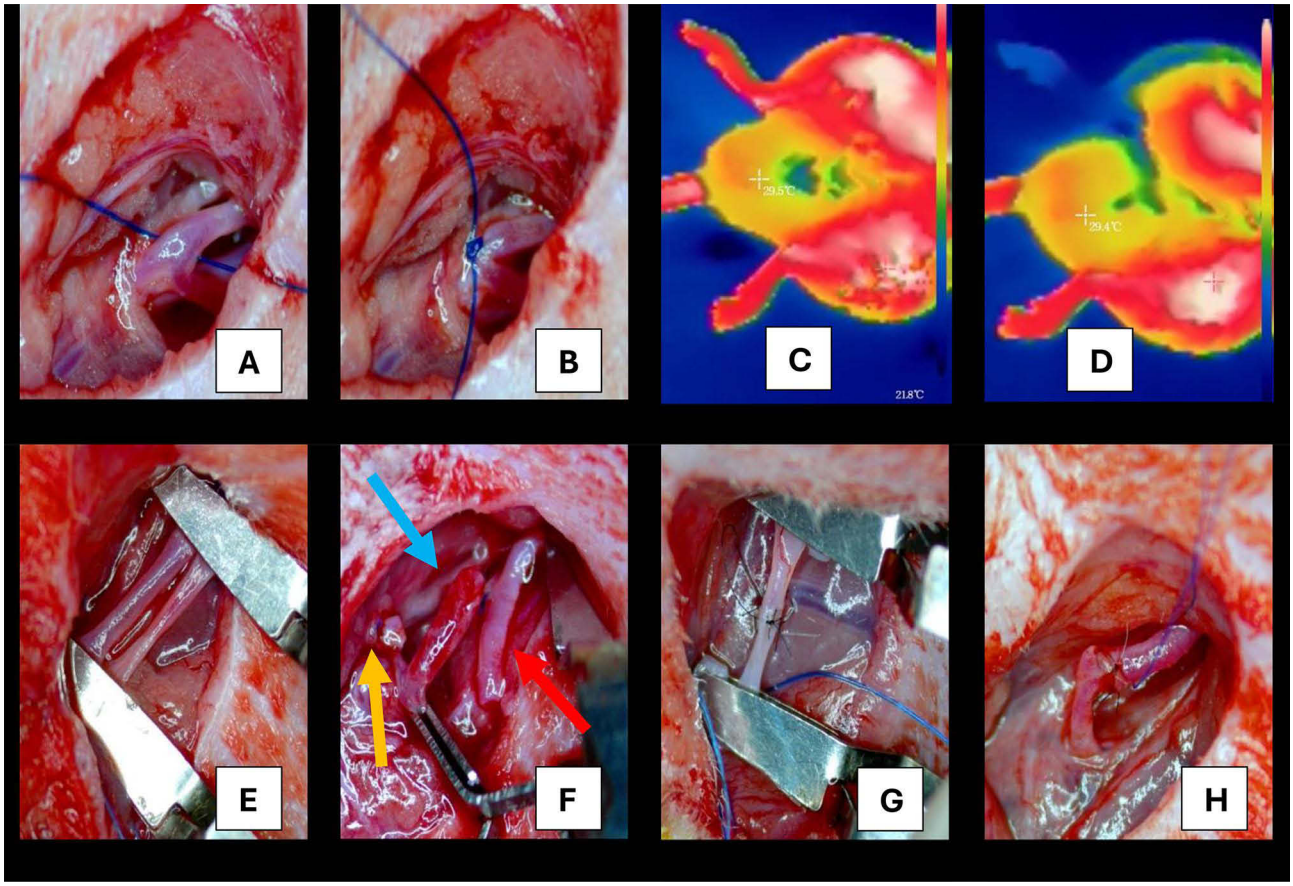

Figure 1 (**A**) CFA identification prior ligation; (**B**) Ligation with 7/0 Polypropylene; (**C** and **D**) Thermal imagin before and after ligation, the right hind limb temperature is significantly lower, marked with blue color (**D**); (**E–H**) Microsurgical technique of Deep Venous Arterialization (DVA). Note, the vein was cut as proximal as possible (blue arrow (**F**)), while the artery was cut as distal as possible (red arrow (**F**)); old artery ligation that was not remove (yellow arrow (**F**)).

Postoperative Clinical Assessment

On postoperative days 2 and 7, animals were observed for clinical signs of ischemia, including skin color changes, coldness, muscle atrophy, wound infection or dehiscence, temperature alteration, and gait impairment. Observations were documented photographically using a smartphone. Functional assessment was performed using the Tarlov score, ischemia score, and modified ischemia score.[17,18] Gait analysis was performed by manual footprint analysis as described by Wertman et al[16] Rats showing infection, wound dehiscence, or death were excluded.

Microsurgical Technique for Distal Venous Arterialization (DVA)

A re-incision was made along the previous surgical line. The ligated artery was identified by locating the polypropylene suture knots. The CFA and FV were carefully dissected and controlled using bulldog clamps placed proximally and distally on both vessels. The artery was transected proximal to the ligation knot, and the vein was transected just distal to the proximal clamp. The proximal venous stump was ligated with 7–0 polypropylene sutures. The distal vein was cannulated with a 0.014" soft cardiac angioplasty wire to disrupt venous valves. The operative field was flushed with 1250 units of heparin in 10 mL saline to prevent coagulation.[19]

An end-to-end arterial–venous anastomosis was created with 10–0 nylon sutures (Ethilon®, BVH100-3, Ethicon) using interrupted sutures (Figure 1E–H). Following anastomosis, distal clamps were released first, followed by proximal clamps. Patency was confirmed by visible pulsation in both artery and vein. Any leakage was corrected with additional sutures. The wound was closed as previously described, followed by immediate postoperative thermal imaging.

Microsurgical Technique for Open Ligation (OL)

For the OL group, the previously ligated CFA was identified by tracing the polypropylene loop suture. The knot was carefully cut using microsurgical scissors to avoid arterial injury. Once the ligature was released, the wound was closed using the same technique, and thermal imaging was performed. The OL group served as an experimental positive control to model restoration of arterial inflow and reperfusion, rather than as a clinically analogous intervention.

Animal Termination and Tissue Harvesting

On day 14, endpoint assessments were performed. Animals first underwent gait analysis, followed by induction of general anesthesia with ketamine–xylazine (intraperitoneal). Infrared thermography was then conducted, after which terminal re-exploration was performed to confirm vascular patency in each group: (i) DVA anastomosis, (ii) arterial patency in the OL group, and (iii) persistence of ligation in the HLI group. While under deep anesthesia, animals were euthanized by intraperitoneal overdose of ketamine–xylazine, in accordance with institutional guidelines.[20] Death was confirmed by loss of reflexes, cessation of spontaneous respiration and heartbeat, and verified by thoracotomy. After a 10-minute postmortem interval, the right gastrocnemius muscle (and contralateral muscle for sham controls) was harvested. Each sample was divided: one portion was snap-frozen in liquid nitrogen and stored at −80 °C, and the other was fixed in 4% neutral-buffered formalin and embedded in paraffin.

Gait Analysis

Gait analysis was performed using manual footprint analysis[16] to assess hindlimb locomotion. Immediately before testing, the plantar surfaces of both hind paws were coated with non-toxic, water-washable paint in contrasting colors (Flomo® washable paint). Rats traversed a transparent tunnel lined with white paper toward a darkened goal box. Paper was replaced between runs. Footprints were digitized and analyzed by a blinded assessor. Primary outcomes were (i) mean stride length for the right and left hindlimbs, and (ii) mean base-of-support (stride width).

Hindlimb Temperature Analysis with Infrared Thermography (IRT)

Intraoperative patency of the DVA anastomosis was verified by direct observation of arterial pulsation within the venous segment and confirmed after wound closure using infrared thermography (IRT; HIKMICRO® Mini1 smartphone module, model HM-TJ11-3AMF-Mini1; Hangzhou Microimage Software). Longitudinal IRT was performed at three time points: baseline (day 1, pre-treatment), day 7 (post-HLI induction), and day 14 (pre-termination). All measurements were performed under standardized room conditions (26°C, no artificial lighting). The examiner handled only the upper body

of rats to avoid heat transfer to the hindlimbs. Thermal images were analyzed in ImageJ v1.54g (NIH). Images were converted to RGB stacks, standardized regions of interest were applied over the hindlimbs, and pixel intensities were calibrated against the embedded scale to yield quantitative temperature values (°C).

Immunohistochemical Analysis for Capillary Density

Capillary density was assessed as a histologic surrogate of angiogenesis.[21–23] Formalin-fixed, paraffin-embedded gastrocnemius sections were stained with a monoclonal anti-CD31 (PECAM-1) antibody (GeneTex, USA; GTX34489). Capillary density was defined as the number of CD31-positive capillaries per mm^2 of muscle fiber area. Five randomly selected fields were analyzed using an Olympus CX21LED microscope and imaged with an Olympus BX51 microscope equipped with a digital camera.

Immunoblotting of HIF-1α, AMPK, LC3, and p62

Western blot analysis was performed to evaluate hypoxia signaling (HIF-1α), energy-sensing pathways (AMPK), and autophagy markers (LC3 and p62/SQSTM1).[10,11,14] Gastrocnemius muscle was homogenized in lysis buffer (10 mM Tris-HCl, 150 mM NaCl, 1 mM EDTA, 1% NP-40, plus protease inhibitors). Lysates were centrifuged, and supernatants were heat-denatured at 96 °C for 5 minutes. Equal amounts of protein (10 μg/lane) were separated by SDS–PAGE and transferred to nitrocellulose membranes (GE Healthcare). Membranes were blocked overnight at 4 °C in 2% blocking solution (GE Healthcare) in TBS-T.

Primary antibodies (Cell Signaling Technology) were used at 1:1000 dilution: anti-HIF-1α (#3716), anti-AMPKα (#2603), anti-LC3 (#12741), anti-p62/SQSTM1 (#8025), and anti-β-actin (#4967). After HRP-conjugated secondary antibody incubation, signals were visualized with enhanced chemiluminescence (GE Healthcare) and imaged using a LI-COR C-DiGit scanner. When required, membranes were stripped (Thermo Scientific) and reprobed for β-actin as a loading control. Densitometry was performed in ImageJ, and protein expression was normalized to β-actin.

Statistical Analysis

Analyses were performed using JASP v0.19 (University of Amsterdam) and Microsoft Excel. Distribution was assessed with the Shapiro–Wilk test (normality for paired data assessed on within-animal differences). Paired, two-tailed *t*-tests were used for left–right comparisons in gait and IRT (background-corrected). Independent two-sample *t*-tests were used for immunohistochemistry and Western blot, with variance homogeneity confirmed by Levene's test. If variance was unequal, Welch's *t*-test was applied. Data are expressed as mean ± SD with 95% confidence intervals. Significance was defined as $p<0.05$ (two-tailed). Data distribution was assessed using the Shapiro–Wilk test. Results are presented as mean ± standard deviation with corresponding effect sizes to enhance interpretability. For molecular analyses (immunohistochemistry and Western blot), tissue samples were randomly selected from each group and were not paired with contralateral limbs on an individual-animal basis. Therefore, these datasets were analyzed as independent samples using unpaired statistical tests.

Ethical Approval

This study complied with the principles of the 3Rs (Replacement, Reduction, Refinement) and the 5Fs (freedoms from hunger and thirst, discomfort, pain, injury, disease, fear/distress, and freedom to express natural behavior). Ethical approval was obtained from the Universitas Padjadjaran Research Ethics Committee (No. 768/UN6.KEP/EC/2022) and the study was registered with AnimalStudyRegistry.org (DOI: 10.17590/asr.0000353).

Results

All animals remained healthy without illness or peri-procedural complications throughout the study period. Mean body weight was 313.7 ± 47 g at baseline (day 0), 310.2 ± 42 g on day 7, and 301.1 ± 23 g on day 14, with no significant change over time ($p = 0.674$). No physical or functional deficits were observed apart from reduced temperature in the right hind limb. Functional assessments yielded Tarlov, ischemia, and modified ischemic scores of 6, 5, and 7, respectively, on day 7 and day 14.[17,18]

Gait Analysis

Measurements were performed on days 0, 7, and 14 (Figure 2C). The parameters assessed included the mean stride length (SL; right versus left) and stride width (SW; right versus left), analyzed separately. All data were normally distributed.

Paired *t*-test analysis (Figure 2A) showed no significant difference in stride length between the left and right limbs on day 0. However, on day 7 a significant reduction was observed (left: 12.9±1.3cm vs. right: 12.2±1.6cm; t=3.252, p=0.003). Similarly, on day 14, the HLI model (control) continued to demonstrate a shorter stride length in the right limb

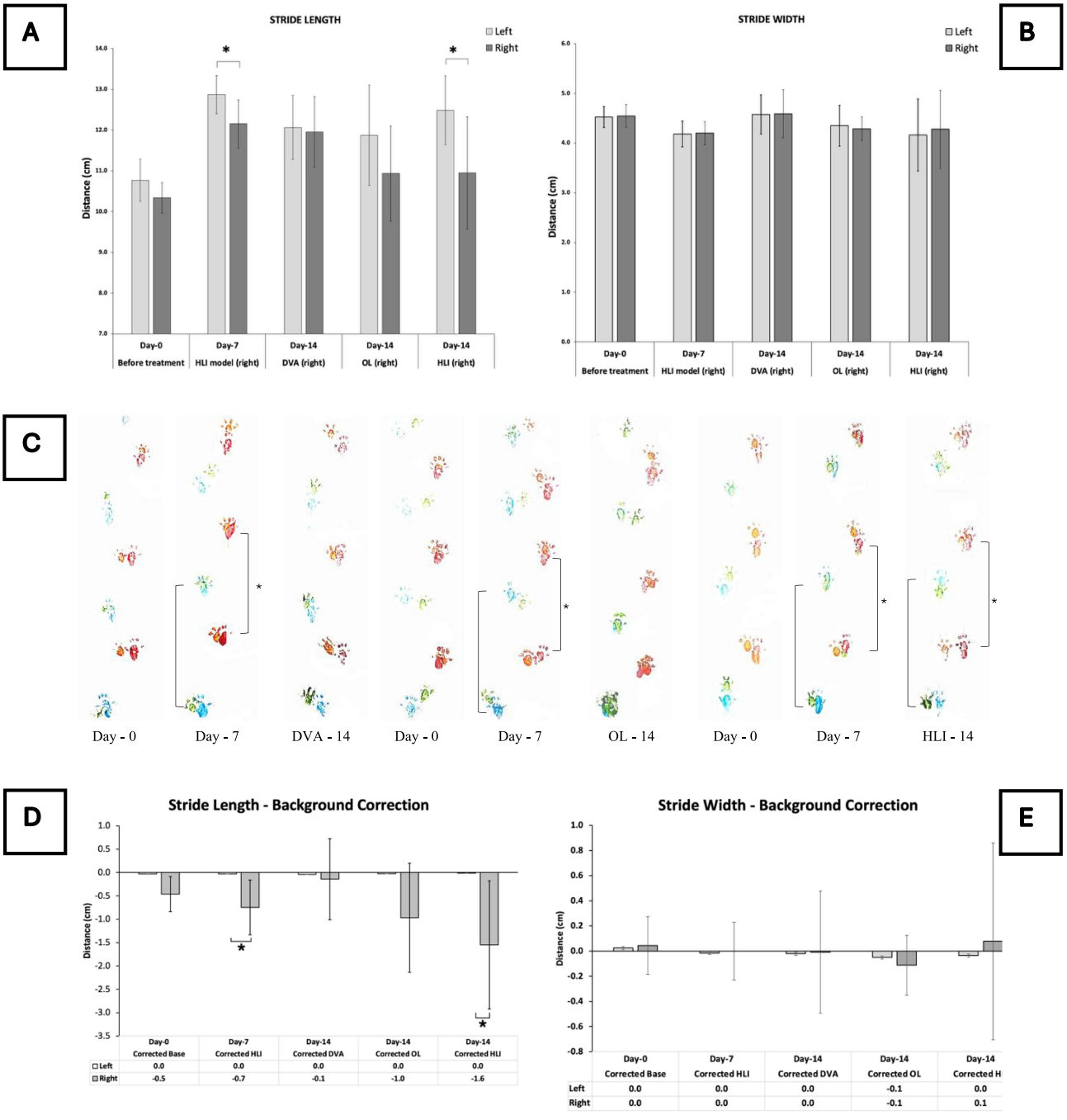

Figure 2 Gait analysis and background-correction. Bar graphs show mean stride length (**A**) and stride width (**B**) differences between the right (ischemic) and left limbs at Day 0, Day 7, and Day 14 across Deep Venous Arterialization (DVA), Open Ligation (OL), and Ligation groups (L groups). The right limb displayed shorter stride length at Days 7 and 14 in the HLI model, whereas no significant asymmetry was observed in DVA or OL groups (**C**). Baseline symmetry (**D** and **E**) was confirmed (p=0.119); significant asymmetry developed at Day 7 (p=0.003) and persisted in L (p=0.004). Bars represent mean ± SD; asterisks indicate p<0.05. For background correction, the contralateral limb of each group is used as the baseline.

(left: 12.3±1.1cm vs. right: 11.0±1.8cm; t=2.729, p=0.034). In contrast, no significant differences were detected in the DVA model (left: 12.1±1.4cm vs. right: 12.0±1.5cm; t=0.257, p=0.802), nor in the OL model (left: 11.9±1.7cm vs. right: 11.0±1.7cm; t=1.365, p=0.214).

For stride width (Figure 2B), paired t-test results indicated no significant differences between the left and right limbs across all models at days 0, 7, and 14 ($p \geq 0.05$).

Background Correction

Baseline gait symmetry (Figure 2D) was confirmed at Day 0 (p=0.119). A significant asymmetry emerged at Day 7 (t=−3.201, p=0.003), indicating ischemic gait disturbance. By Day 14, the DVA group achieved full restoration of symmetry (p=0.805), while the OL group showed mild, non-significant improvement (p=0.227). In contrast, the L group remained significantly asymmetric (t=4.452, p=0.004), reflecting persistent ischemic dysfunction. Paired-sample analysis of background-corrected stride width (Figure 2E) revealed no significant right–left differences at any time point (all p>0.05). Mean ΔStride values were minimal (≤0.1 cm), indicating overall gait symmetry, with only the Day 14 L group showing a slight, non-significant tendency toward longer right-limb strides (p=0.130).

Infrared Thermography Analysis

Prior to surgery, temperatures of the left and right hind limbs were measured (Figure 3C). The Wilcoxon test (non-normally distributed data) showed no significant difference between limbs (left: 33.8±1.3°C vs. right: 33.6±1.0°C; z=1.727, p=0.086). However, on day 7 after the establishment of the HLI model (Figure 3A), a significant temperature difference was observed (left: 33.8±1.9°C vs. right: 28.9±2.0°C; z=4.782, p<0.001).

On day 14 (Figure 3A and D), the DVA model did not demonstrate any significant temperature differences between the left and right limbs (left: 32.7±2.4°C vs. right: 32.4±2.1°C; z=0.157, p=0.910), nor did the OL model (left: 32.9 ±2.2°C vs. right: 32.1±2.6°C; t=1.447, p=0.191). In contrast, the HLI model exhibited a significant difference (left: 34.9 ±0.5°C vs. right: 30.4±1.8°C; t=7.623, p<0.001).

Background Correction

Paired-sample and Wilcoxon signed-rank analysis revealed no significant thermal asymmetry at baseline (contralateral limb - Day 0, p=0.227 (Figure 3B)). Following ischemia induction, a marked right–left temperature difference was observed at Day 7 (t=11.599, p<0.001), indicating significant hypothermia of the ischemic limb. By Day 14, thermal symmetry was restored in the DVA group (p=0.681), while the OL group showed mild, non-significant improvement (p=0.191). In contrast, the L/HLI group maintained a pronounced temperature deficit (t=7.623, p<0.001), consistent with persistent ischemic hypoperfusion.

Immunohistochemical Analysis for Capillary Density

Muscle samples were obtained on day 14 (Figure 4A–D). All data were normally distributed, except for the sham group. The HLI (L) model demonstrated a significant increase in capillary density compared with sham (U=10.000, p=0.031). In contrast, the DVA group showed a significant reduction compared with HLI (t=3.184, p=0.004), as did the OL group (t=2.951, p=0.007) (Figure 4A).

Western Blot Analysis

Western blot analysis was performed to assess the relative expression ratios of HIF-1α, AMPK, LC3-II, and p62 proteins in skeletal muscle samples on day 14.

HIF-1α (Figure 5A). The HLI group exhibited the highest HIF-1α protein expression compared with all other groups, with a significant increase relative to the sham group (0.730±0.3 vs. 0.371±0.1; U=2.000, p=0.016). Neither the DVA group (0.488±0.2; U=8.000, p=0.210) nor the OL group (0.517±0.2; U=9.000, p=0.274) differed significantly from sham. Likewise, the decreases observed in the DVA and OL groups relative to HLI did not reach statistical significance (U=20.000, p=0.075 and U=19.000, p=0.111, respectively).

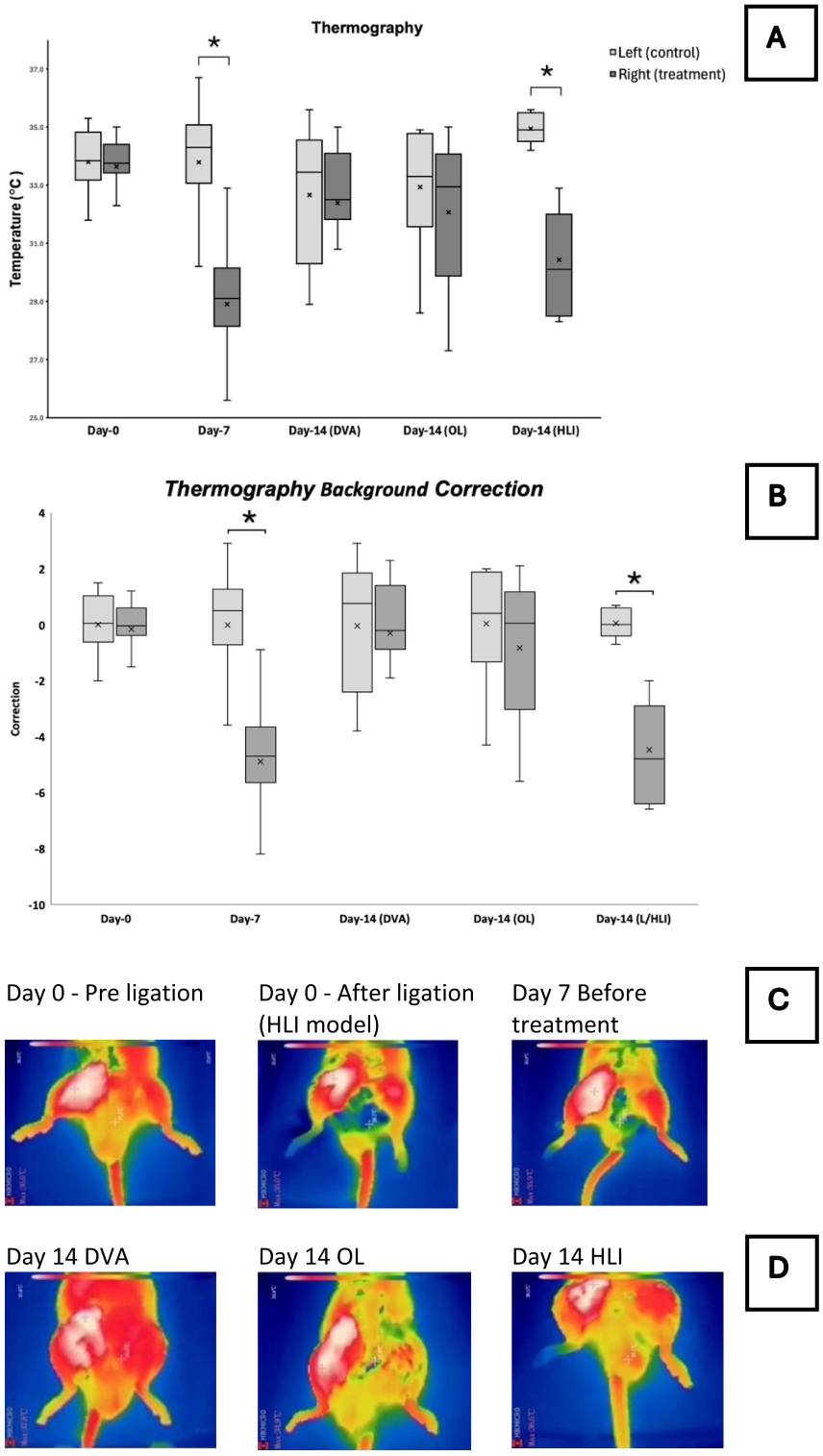

Figure 3 Infrared Thermographic Assessment of Hindlimb Ischemia and Temperature Recovery Following Deep Venous Arterialization. (**A**) Infrared thermography of hindlimb temperature. In the Hind Limb Ishcemia (HLI) model, the right limb showed a significant reduction in temperature compared with the left at days 7 and 14, while no asymmetry was observed in the Deep Venous Arterialization (DVA) or Open Ligation (OL) models. Figure 1C and D are the Representative images of infrared thermography. (**B**) Background correction Box plot showing mean right–left limb temperature differences at Day 0, Day 7, and Day 14. Ische-mic hypothermia appeared at Day 7, recovered in Deep Venous Arterialization (DVA), partially improved in Open Ligation (OL), and persisted in Ligation (L) Hind Limb Ischemia (HLI). The contralateral limb of each group is used as the baseline. (**C**) The HLI model creation. The right hind limb temperature is significantly reduced. (**D**) The temperature on day 14. Deep Venous Arterialization (DVA) and Open Ligation (OL) resumed to its normal temperature, while the Hind Limb Ischemia (HLI) remain cold.
Note: *p < 0.05 vs contralateral limb at the same time point.

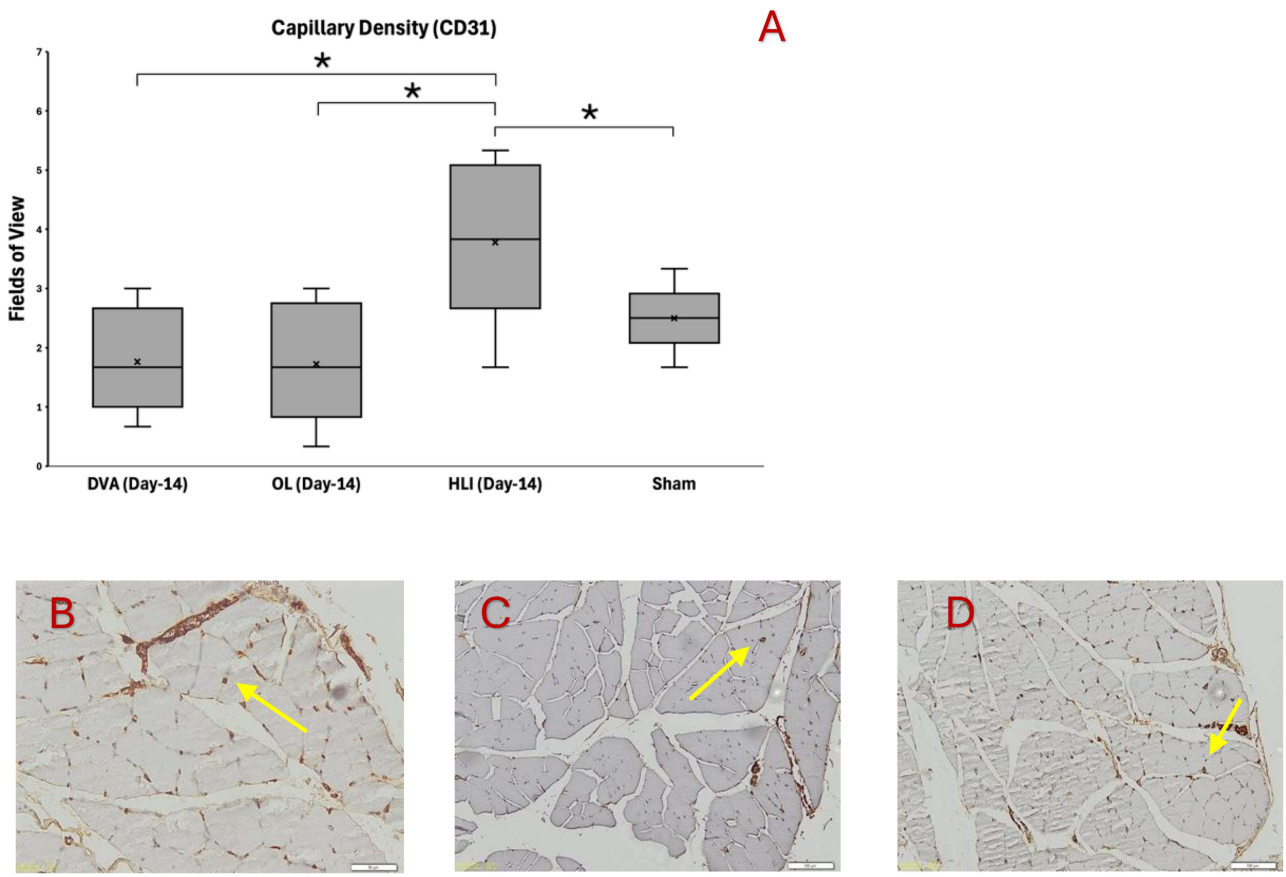

Figure 4 Capillary Density Analysis Capillary density was significantly higher in the Hind Limb Ischemia (HLI) (L) group compared with sham (p=0.031). Both Deep Venous Arteliazation (DVA) (p=0.004) and Open Ligation (OL) (p=0.007) groups showed significant reductions compared with HLI. Capillary density immunostaining (CD31) in a skeletal muscle on day 14. Representative images from Hind Limb Ischemia (HLI) (**B**), Deep Venous Arterialization (DVA) (**C**), and Sham (**D**) are shown.
Note: (**A**) *p < 0.05 (statistically significant difference between the indicated groups). Arrows in (**B–D**) Arrows indicate CD31-positive capillary structures used for density quantification.

AMPK (Figure 5B). The HLI group also showed the highest AMPK protein expression, which was significantly increased compared with sham (0.855±0.3 vs. 0.457±0.2; t=2.728, p=0.011). In contrast, DVA (0.549±0.3; t=−0.691, p=0.505) and OL (0.452±0.3; t=0.036, p= 0.972) did not differ significantly from sham. However, both groups demonstrated significantly lower AMPK expression compared with HLI (DVA: t=1.884, p=0.044; OL: t=2.429, p=0.018).

p62 (Figure 5C). Protein expression of p62 did not differ significantly among groups (p>0.05). The HLI group demonstrated the lowest expression (0.556±0.1) compared with DVA (0.619±0.2) and sham (0.740±0.2), while the OL group (0.745±0.3) showed a slight, nonsignificant increase relative to sham.

LC3-II (Figure 5D). The DVA group demonstrated the lowest LC3-II expression (0.301±0.1) compared with sham (0.673 ±0.2) and HLI (0.801±0.5), with statistically significant reductions (t =2.116, p=0.032 and t=3.819, p=0.002, respectively). In contrast, the OL group (0.570±0.3) showed nonsignificant decreases compared with sham (t_{Welch}=0.650, p=0.267) and HLI (t=0.924, p=0.189).

Discussion

This study evaluated functional, vascular, and molecular adaptations of ischemic skeletal muscle following distal venous arterialization (DVA) in a rat hindlimb ischemia model, with particular focus on autophagy-related signaling.

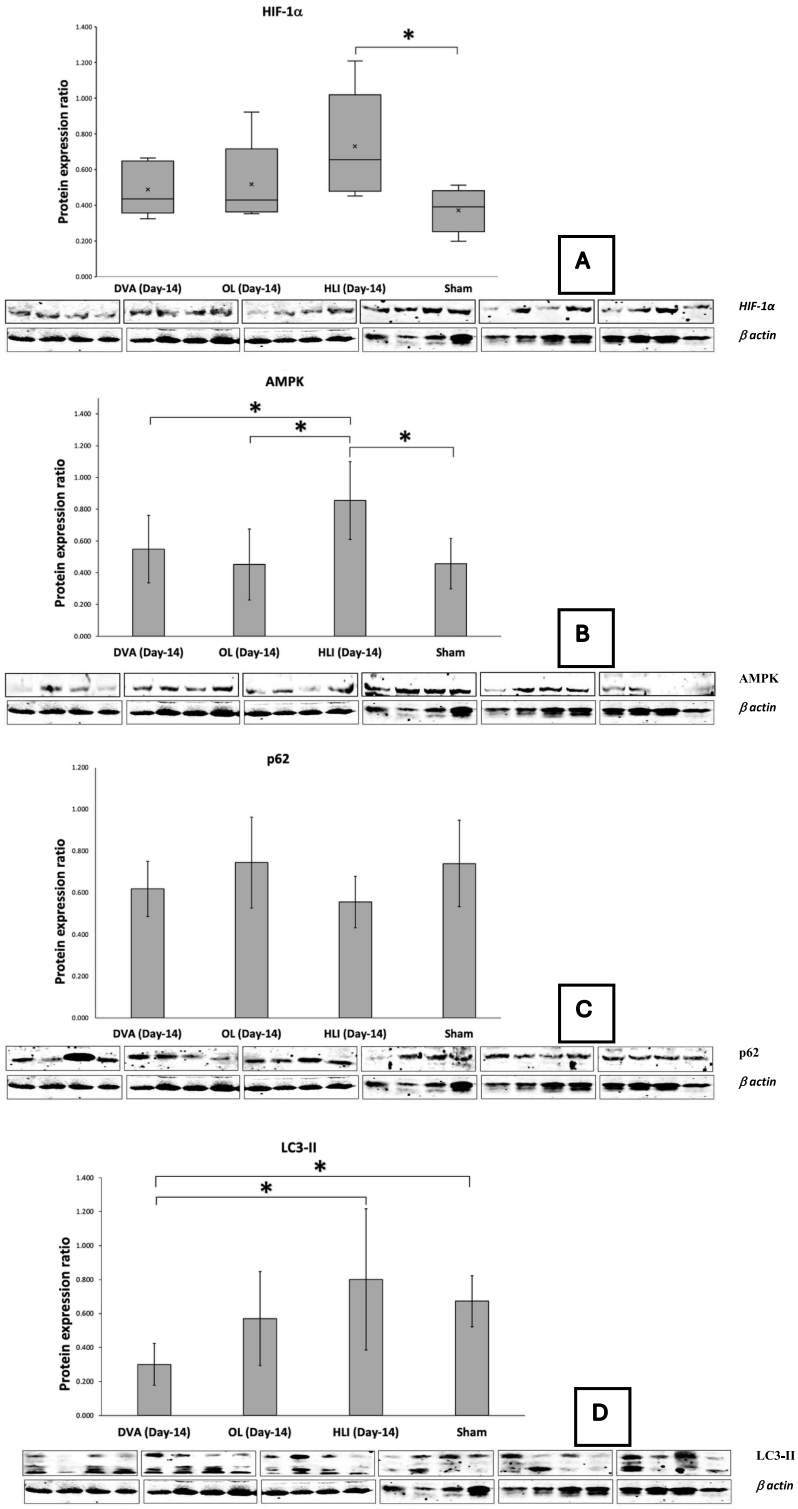

Figure 5 Deep Venous Arterialization Modulates Hypoxia and Autophagy-Related Protein Expression Following Hindlimb Ischemia. (**A**) Western Blot HIF-1α: Hind Limb Ischemia (HLI) (0.730±0.3) was significantly increased compared with sham (0.371±0.1; p=0.016). Deep Venous Arterialization (DVA) (0.488±0.2) and Open Ligation (OL) (0.517±0.2) did not differ from sham (p>0.05). (**B**) Western Blot. AMPK: Hind Limb Ischemia (HLI) (0.855±0.3) was significantly higher than sham (0.457±0.2; p=0.011). Deep Venous Arterialization (DVA) (0.549±0.3) and and Open Ligation (OL) (0.452±0.3) were not different from sham (p>0.05), but both were significantly lower than HLI (p<0.05). (**C**) Western Blot. p62: No significant differences were observed among groups (p>0.05), with lowest expression in Hind Limb Ischemia (HLI) (0.556±0.1) versus Deep Venous Arterialization (DVA) (0.619±0.2), sham (0.740±0.2), and Open Ligation (OL) (0.745±0.3). (**D**) Western Blot. LC3-II: Deep Venous Arterialization (DVA) (0.301±0.1) showed the lowest expression, with significant reductions versus sham (0.673±0.2; p=0.032) and Hind Limb Ischemia (HLI) (0.801±0.5; p=0.002). OL (0.570±0.3) showed nonsignificant decreases compared with sham and HLI (p>0.05).

Gait Function

Following the induction of HLI, none of the extremities exhibited overt physical damage such as necrosis, gangrene, or autoamputation, despite ligation of the right common femoral artery. This confirms that the model successfully produced ischemia without severe limb destruction, thereby serving as an appropriate experimental HLI model.[17,22,24,25]

Generally, hindlimb muscle injury (non-ischemic) reduces stride length on day 3, which begins to recover by day 7.[26] Consistent with other studies, HLI induction in Wistar rats via femoral artery ligation and excision leads to altered gait, including prolonged swing phase and shortened stride length (SL).[27–29] Interestingly, human studies on peripheral artery disease (PAD) gait parameters remain inconsistent. Human gait studies in PAD show heterogeneous findings, likely due to confounding factors such as fitness and disease severity.[30,31]

In the present study, the right hindlimb displayed a significantly shorter stride length than the left on day 7 after HLI induction (p=0.029). By day 14, after DVA or OL procedures, this difference was no longer significant (p=0.422 and p=0.140, respectively). Conversely, the HLI group continued to show a significant reduction in stride length (p=0.041). These findings suggest that HLI induces gait impairment manifested as shortened stride length, which improves following revascularization (DVA and OL) but persists in the ligation-only model. In contrast, stride width did not differ significantly in any group, either at day 7 or day 14. To our knowledge, no prior studies have specifically investigated the impact of DVA on gait in rodents (PubMed, Google Scholar).

Infrared Thermography Analysis

Infrared thermography (IRT) provides a non-invasive estimate of surface temperature and tissue perfusion and has been used to monitor ischemia and reperfusion in both clinical and experimental settings.[32–36]

IRT has been increasingly applied in lower-limb ischemia for both diagnostic purposes and monitoring revascularization outcomes in acute limb ischemia (ALI) and chronic limb-threatening ischemia (CLTI).[32–35] In rodent models, IRT effectively detects ischemia: femoral artery clamping induces rapid limb cooling, followed by temperature recovery upon reperfusion.[37] Other mouse studies confirm sharp temperature drops after ligation with gradual, non-significant recovery up to day 28.[35,37–39] Smartphone-based IRT studies similarly show persistent ischemia at day 7 in controls, with improved perfusion in treated groups.[40,41]

Our study demonstrated a significant temperature decline in created HLI model at day 7 (28.9±2.0°C) compared with pre-ligation (33.6±1.0°C) and controls (33.8±1.9°C). By day 14, HLI group remained significantly cooler (30.4±1.8°C vs. 34.9±0.5°C, p<0.05). In contrast, DVA and OL groups showed temperature restoration approaching contralateral limbs (DVA: 32.4±2.1°C vs. 32.7±2.4°C; OL: 32.1±2.6°C vs. 32.9±2.2°C). These results corroborate previous reports on the diagnostic and follow-up utility of IRT in ischemia and reperfusion models.[37] Notably, no prior literature on IRT in DVA models was identified.

Capillary Density

Capillary density, assessed by CD31 immunohistochemistry, reflects angiogenesis. Prior rodent studies reported significant increases in capillary density following femoral artery ligation.[18,21,42–44] In one unique experiment, capillary density increased in HLI alone but decreased in HLI with denervation or denervation only, suggesting a modulatory role of peripheral nerves in arteriogenesis.[45] Contrastingly, human studies in lower extremity arterial disease (LEAD/PAD) revealed reduced capillary density in gastrocnemius biopsies,[46–48] although some earlier reports found elevated density, suggesting compensatory mechanisms.[47,49,50]

Reperfusion injury introduces additional complexity, as prolonged ischemia and inflammatory mediators can impair tissue and vascular responses.[51–54] Rodent tourniquet studies showed non-significant changes in capillary density after reperfusion.[55] More recent studies with collateral-dependent reperfusion also reported no density changes up to 90 days.[56,57]

In the current study, capillary density increased significantly in HLI compared with sham (p=0.031). However, both DVA and OL groups exhibited significant decreases compared with HLI, though values were not significantly different from sham. This suggests that revascularization normalizes capillary density levels, consistent with previous findings.[58] The discrepancy

between rodent and human data likely reflects differences between acute experimental ischemia and chronic human disease. Importantly, no comparable data for DVA models were identified.

HIF-1α Expression

HIF-1α is a master regulator of hypoxia-mediated cellular adaptation.[10,11,59] Its expression increases under ischemia and reperfusion injury, often triggering autophagy.[10] Prior studies consistently demonstrate HIF-1α upregulation under ischemic conditions.[21,60] In a sildenafil study, HIF-1α increased in HLI controls but remained normal with treatment, despite unchanged capillary density.[61] Mouse models similarly show early increases in HIF-1α (day 3), persisting but reduced by day 14, and correlating with increased capillary density.[62,63]

Our study found significantly elevated HIF-1α expression in HLI compared with sham at day 14 (p=0.016), consistent with previous reports.[61–63] DVA and OL groups, however, showed no significant increases compared with sham (p>0.05), indicating that revascularization may inhibit HIF-1α activation. This aligns with our capillary density findings, supporting the role of hypoxia-driven HIF-1α signaling in angiogenesis.[21,62,63]

AMPK Expression

AMP-activated protein kinase (AMPK) is a central regulator of cellular metabolism, activated under low intracellular ATP (eg., hypoxia). Increased AMP/ATP ratio triggers AMPK activation independently of HIF-1α.[14] As a "metabolic checkpoint," AMPK suppresses mTORC1 activity, thereby promoting autophagy.[64,65] Rodent studies show HLI-induced AMPK activation coincides with increased capillary density, highlighting its role in ischemia-induced angiogenesis.[66,67]

In this study, AMPK expression increased significantly in HLI compared with sham, while DVA and OL groups demonstrated significant reductions toward sham values. These findings suggest an association between ischemia, AMPK activation, and metabolic stress, with normalization following revascularization.[67]

p62 and LC3-II Expression

Autophagy can be evaluated via p62 (sequestosome-1) and LC3 (microtubule-associated protein 1A/1B light chain 3), both widely recognized autophagosome markers.[8,68–73] LC3-II localizes to autophagosome membranes, while p62 is degraded during autophagic flux.[74]

Rodent models show dynamic expression: LC3-II increases on day 7, while p62 rises on day 3 and declines by day 7.[75] Other studies report stable LC3-II/LC3-I ratios in chronic HLI unless exercise is introduced,[74] or reduced LC3-II after reperfusion with concomitant p62 decline.[76] Additional evidence supports decreased p62 and increased LC3 in ischemia, alongside elevated HIF-1α and CD31.[70] By day 28, LC3-II levels typically normalize.[65] Human PAD studies confirm higher LC3 and capillary density, with reduced plasma p62 indicating enhanced autophagy.[54,77,78]

In our study, LC3-II expression increased in HLI but not significantly compared with sham (p=0,287). Interestingly, DVA significantly reduced LC3-II compared with both sham and HLI (p=0.032; p=0,002), indicating suppressed autophagy. p62 expression decreased in HLI versus sham, though not significantly (p=0.083), and increased in DVA and OL compared with HLI, again without significance. While not statistically robust, these findings suggest potential modulation of autophagy via p62 signaling in chronic ischemia. Collectively, the observed AMPK elevation in HLI and reduction in DVA further support these mechanistic links. Therefore, the observed changes in LC3-II and p62 should be interpreted as alterations in autophagy-related markers rather than definitive evidence of altered autophagic flux.

Overall Interpretation

Overall, this study demonstrates that prolonged hindlimb ischemia leads to reduced oxygen delivery, metabolic shift to anaerobic respiration, and increased AMP/ATP ratio, manifested as limb cooling, elevated capillary density, impaired gait, and upregulation of HIF-1α and AMPK, with a corresponding increase in autophagy marker (LC3-II). In contrast, distal venous arterialization restored perfusion, normalized temperature and capillary density, and improved gait, accompanied by reductions in HIF-1α, AMPK, and LC3-II toward sham levels. These changes suggest that DVA was associated with normalization of hypoxia-related signaling and reductions in autophagy-related markers. Together, the functional, thermal, vascular, and molecular outcomes highlight both the pathological cascade induced by ischemia and

the physiological recovery achieved through DVA, supporting its role as a potential revascularization strategy for ischemic skeletal muscle. From a translational perspective, these findings provide mechanistic support for the clinical use of distal venous arterialization in chronic limb-threatening ischemia with no other option. Demonstrating improvements in functional performance, tissue perfusion, and molecular markers of hypoxia and autophagy helps bridge the gap between observed clinical limb salvage outcomes and their underlying biological mechanisms. These data therefore strengthen the biological plausibility of DVA as a revascularization strategy for ischemic skeletal muscle.

Study Limitations and Future Directions

This study has several important limitations. The HLI model, based on femoral artery ligation without collateral excision, may have permitted residual collateralization and thus does not fully replicate the chronic progression of PAD/CLTI in humans, for which no ideal animal model currently exists.[17,21,22,24,25,79–81] The use of relatively young, otherwise healthy rats without comorbidities such as diabetes or vascular disease further limits translational relevance, as age and comorbidity strongly influence ischemic recovery.[18,22,24,25]

In addition, the marked difference in operative time between DVA and OL could have introduced bias through prolonged anesthesia and surgical stress, while analgesia and stress biomarkers were insufficiently evaluated. Methodological constraints such as tissue sampling limited to day 14, variability in gait analysis, and the lower accuracy of infrared thermography compared with Laser Doppler Perfusion Imaging also reduce the robustness of the findings. Infrared thermography provides an indirect estimate of perfusion and may be influenced by ambient temperature or handling despite standardization. The small sample size and scarcity of comparative literature on autophagy in PAD and on DVA in animal models further restrict generalizability. Because autophagic flux and AMPK activation status were not directly measured, these findings should be interpreted as associations rather than definitive causal mechanisms.

Future studies should aim to employ older animals or models with relevant comorbidities, extend observation periods beyond 14 days to better approximate chronic ischemia, and incorporate more precise tools such as treadmill-based gait systems and Laser Doppler Perfusion Imaging. Standardizing operative times, expanding sample sizes, and integrating stress biomarkers could also strengthen validity. Ultimately, the development of more clinically relevant animal models will be essential to bridge the translational gap between experimental research and human PAD/CLTI. The relatively small and unequal group sizes, particularly the larger DVA group due to technical considerations of microsurgery, may have limited statistical power and could affect the generalizability of the findings. In addition, molecular analyses were performed at a single endpoint (day 14), which may not fully capture the temporal dynamics of autophagy regulation.

Conclusion

In this study, distal venous arterialization (DVA) in a rat hindlimb ischemia model restored gait function and normalized limb temperature without inducing severe complications such as gangrene. DVA was associated with improvement of ischemia-related skeletal muscle changes, including normalization of capillary density and reductions in hypoxia-related markers (HIF-1α, AMPK). Furthermore, DVA was accompanied by lower expression of the autophagy-related marker LC3-II, while p62 remained unchanged. These findings suggest that DVA promotes functional and suggesting molecular recovery in ischemic skeletal muscle and represents a promising revascularization strategy.

Use of Artificial Intelligence

The authors acknowledge the use of ChatGPT (OpenAI, San Francisco, CA, USA) to assist with language editing and improving the clarity of the manuscript. All content generated using this tool was carefully reviewed, verified, and edited by the authors, who take full responsibility for the integrity and accuracy of the final version.

Highlights

- Distal venous arterialization (DVA) restored gait function and normalized hindlimb temperature in a rat ischemia model.
- DVA reversed ischemic muscle changes, with capillary density returning to sham levels.
- Hypoxia-driven signaling (HIF-1α, AMPK) was suppressed after DVA, reducing excessive autophagy.

- LC3-II expression decreased following DVA, while p62 remained unaffected.
- DVA represents a feasible revascularization approach that promotes functional and molecular recovery in ischemic skeletal muscle.

Acknowledgments

The authors gratefully acknowledge Ms. Mia Zahrotul Munawaroh, Ms. Putri Sifa Lestari, and Ms. Syafira (Animal Laboratory, Universitas Padjadjaran) for animal handling, Mrs. Susianti and Ms. Canadia Ravelita (Central Laboratory, Universitas Padjadjaran) for Western blot assistance, and Mr. Herman (Department of Pathology, Hasan Sadikin Hospital) for technical support. The authors also thank Dr. Rani Septrina and dr. Jonathan Mark for their valuable support. This study was funded by Universitas Padjadjaran Internal Research Grant No. 1595/UN6.3.1/PT.00/2021.

This publication charge is funded by Unpad through the *Indonesian Endowment Fund for Education* (LPDP) on behalf of the Indonesian Ministry of Higher Education, Science and Technology and managed under the EQUITY Program (Contract No. 4303/B3/DT.03.08/2025 and 3927/UN6. RKT/HK.07.00/2025).

Disclosure

The authors declare no conflicts of interest in this work.

References

1. Lin J, Chen Y, Jiang N, Li Z, Xu S. Burden of peripheral artery disease and its attributable risk factors in 204 countries and territories from 1990 to 2019. *Front Cardiovasc Med*. 2022;9:868370. doi:10.3389/fcvm.2022.868370
2. Abola MTB, Golledge J, Miyata T, et al. Asia-Pacific Consensus Statement on the Management of Peripheral Artery Disease: a Report from the Asian Pacific Society of Atherosclerosis and Vascular Disease Asia-Pacific Peripheral Artery Disease Consensus Statement Project Committee. *J Atheroscler Thromb*. 2020;27(8):809–907. doi:10.5551/jat.53660
3. Aboyans V, Ricco JB, Bartelink MEL, et al; ESC Scientific Document Group. 2017 ESC guidelines on the diagnosis and treatment of peripheral arterial diseases, in collaboration with the European Society for Vascular Surgery (ESVS). *Eur Heart J*. 2018;39(9):763–816. doi:10.1093/eurheartj/ehx095
4. Zemaitis MR, Boll JM, Dreyer MA. Peripheral arterial disease. In: *StatPearls [Internet]*. Treasure Island (FL): StatPearls Publishing; 2023.
5. The Global Lower Extremity Amputation Study Group. Epidemiology of lower extremity amputation in centres in Europe, North America and East Asia. *Br J Surg*. 2000;87(3):328–337. doi:10.1046/j.1365-2168.2000.01344.x
6. Lu XW, Idu MM, Ubbink DT, Legemate DA. Meta-analysis of the clinical effectiveness of venous arterialization for salvage of critically ischaemic limbs. *Eur J Vasc Endovasc Surg*. 2006;31(5):493–499. doi:10.1016/j.ejvs.2005.12.017
7. Schreve MA, Vos CG, Vahl AC, et al. Venous arterialisation for salvage of critically ischaemic limbs: a systematic review and meta-analysis. *Eur J Vasc Endovasc Surg*. 2017;53(3):387–402. PMID: 28027892. doi:10.1016/j.ejvs.2016.11.007
8. Denton D, Kumar S. Autophagy-dependent cell death. *Cell Death Differ*. 2019;26(4):605–616. PMID: 30568239; PMCID: PMC6460387. doi:10.1038/s41418-018-0252-y
9. Kang C, Ji LL. Role of PGC-1α signaling in skeletal muscle health and disease. *Ann NY Acad Sci*. 2012;1271:110–117. doi:10.1111/j.1749-6632.2012.06738.x
10. Pisani DF, Dechesne CA. Skeletal muscle HIF-1α expression is dependent on muscle fiber type. *J Gen Physiol*. 2005;126(2):173–178. doi:10.1085/jgp.200509265
11. Favier FB, Britto FA, Freyssenet DG, Bigard XA, Benoits H. HIF-1-driven skeletal muscle adaptations to chronic hypoxia: molecular insights into muscle physiology. *Cell Mol Life Sci*. 2015;72(24):4681–4696. doi:10.1007/s00018-015-2025-9
12. Wang L, Jin Z, Wang J, et al. Detrimental effect of hypoxia-inducible factor-1α-induced autophagy on multiterritory perforator flap survival in rats. *Sci Rep*. 2017;7(1):11791. PMID: 28924179; PMCID: PMC5603514. doi:10.1038/s41598-017-12034-x
13. Li L, Tan J, Miao Y, Lei P, Zhang Q. ROS and autophagy: interactions and molecular regulatory mechanisms. *Cell Mol Neurobiol*. 2015;35(5):615–621. PMID: 25722131; PMCID: PMC11486209. doi:10.1007/s10571-015-0166-x
14. Dengler F. Activation of AMPK under hypoxia: many roads leading to Rome. *Int J Mol Sci*. 2020;21(7):2428. PMID: 32244507; PMCID: PMC7177550. doi:10.3390/ijms21072428
15. Jung S, Jeong H, Yu SW. Autophagy as a decisive process for cell death. *Exp Mol Med*. 2020;52(6):921–930. PMID: 32591647; PMCID: PMC7338414. doi:10.1038/s12276-020-0455-4
16. Wertman V, Gromova A, La Spada AR, Cortes CJ. Low-cost gait analysis for behavioral phenotyping of mouse models of neuromuscular disease. *J Vis Exp*. 2019;149:e59878. doi:10.3791/59878
17. Brenes RA, Jadlowiec CC, Bear M, et al. Toward a mouse model of hind limb ischemia to test therapeutic angiogenesis. *J Vasc Surg*. 2012;56:1669–1679. doi:10.1016/j.jvs.2012.04.067
18. Westvik TS, Fitzgerald TN, Muto A, et al. Limb ischemia after iliac ligation in aged mice stimulates angiogenesis without arteriogenesis. *J Vasc Surg*. 2009;49(2):464–473. doi:10.1016/j.jvs.2008.08.077
19. Portilla-de-buen E, Ramos E, Leal L, et al. Activated clotting time and heparin administration in Sprague-Dawley rats and Syrian golden hamsters. *Contemp Top Lab Anim Sci*. 2004;43(2):21–24. PMID: 15053503.
20. American Veterinary Medical Association. *AVMA Guidelines for the Euthanasia of Animals: 2020 Edition*. Schaumburg (IL): AVMA; 2020:35.

21. Yang Y, Tang G, Yan J, et al. Cellular and molecular mechanism regulating blood flow recovery in acute versus gradual femoral artery occlusion are distinct in the mouse. *J Vasc Surg*. 2008;48(6):1546–1558. doi:10.1016/j.jvs.2008.07.063
22. Lotfi S, Patel AS, Mattock K, Egginton S, Smith A, Modarai B. Towards a more relevant hind limb model of muscle ischaemia. *Atherosclerosis*. 2013;227:1–8. doi:10.1016/j.atherosclerosis.2012.10.060
23. Dokun AO, Keum S, Hazarika S, et al. A quantitative trait locus (LSq-1) on mouse chromosome 7 is linked to the absence of tissue loss after surgical hindlimb ischemia. *Circulation*. 2008;117(9):1207–1215. doi:10.1161/CIRCULATIONAHA.107.736447
24. Lejay A, Choquet P, Thaveau F, et al. A new murine model of sustainable and durable chronic critical limb ischemia fairly mimicking human pathology. *Eur J Vasc Endovasc Surg*. 2015;49:205–212.
25. Hoinoiu B, Jiga LP, Nistor A, et al. Chronic hindlimb ischemia assessment; quantitative evaluation using laser doppler in a rodent model of surgically induced peripheral arterial occlusion. *Diagnostics*. 2019;9(4):139. doi:10.3390/diagnostics9040139
26. Lu YH, Huang YF, Hsieh CP, Chen JK, Chen HY, Chuang SM. Betulin accelerated the functional recovery of injured muscle in a mouse model of muscle contusion. *Int J Med Sci*. 2024;21(1):37–44. PMID: 38164348; PMCID: PMC10750331. doi:10.7150/ijms.87649
27. Luque Contreras D, Jiménez Estrada I, Martínez Fong D, et al. Hindlimb claudication reflects impaired nitric oxide-dependent revascularization after ischemia. *Vascul Pharmacol*. 2007;46(1):10–15. PMID: 17011243. doi:10.1016/j.vph.2006.06.017
28. Guo L, Yang Q, Wei R, et al. Enhanced pericyte-endothelial interactions through NO-boosted extracellular vesicles drive revascularization in a mouse model of ischemic injury. *Nat Commun*. 2023;14:7334. doi:10.1038/s41467-023-43153-x
29. Ohno K, Tomizawa A, Mizuno M, Jakubowski JA, Sugidachi A. Prasugrel, a platelet P2Y12 receptor antagonist, improves abnormal gait in a novel murine model of thrombotic hindlimb ischemia. *J Am Heart Assoc*. 2016;5(4):e002889. PMID: 27053057; PMCID: PMC4859280. doi:10.1161/JAHA.115.002889
30. McCamley JD, Cutler EL, Schmid KK, et al. Gait mechanics differences between healthy controls and patients with peripheral artery disease after adjusting for gait velocity stride length and step width. *J Appl Biomech*. 2019;35(1):19–24. PMID: 29989479; PMCID: PMC6328338. doi:10.1123/jab.2017-0257
31. Toosizadeh N, Stocker H, Thiede R, Mohler J, Mills JL, Najafi B. Alterations in gait parameters with peripheral artery disease: the importance of pre-frailty as a confounding variable. *Vasc Med*. 2016;21(6):520–527. PMID: 27634957; PMCID: PMC6647841. doi:10.1177/1358863X16660626
32. Vasilev S, Petrov I, Stankov Z, Janevska L, Adam G. Infrared thermography imaging as a diagnostic tool in the case of acute lower limb ischemia. *Bulgarian Cardiol*. 2022;28(3):106–110. doi:10.3897/bgcardio.28.e91048
33. Pakarinen T, Joutsen A, Oksala N, Vehkaoja A. Assessment of chronic limb threatening ischemia using thermal imaging. *J Therm Biol*. 2023;112:103467. PMID: 36796912. doi:10.1016/j.jtherbio.2023.103467
34. Zenunaj G, Lamberti N, Manfredini F, et al. Infrared thermography as a diagnostic tool for the assessment of patients with symptomatic peripheral arterial disease undergoing infrafemoral endovascular revascularisations. *Diagnostics*. 2021;11(9):1701. PMID: 34574042; PMCID: PMC8469591. doi:10.3390/diagnostics11091701
35. Verduzco-Mendoza A, Bueno-Nava A, Wang D, et al. Experimental applications and factors involved in validating thermal windows using infrared thermography to assess the health and thermostability of laboratory animals. *Animals*. 2021;11(12):3448. PMID: 34944225; PMCID: PMC8698170. doi:10.3390/ani11123448
36. Gururajarao SB, Venkatappa U, Shiviram JM, Sikandar MY, Amoudi AA. Chapter 4 - infrared thermography and soft computing for diabetic foot assessment. In: Dey N, Borra S, Ashour AS, Shi F, editors. *Machine Learning in Bio-Signal Analysis and Diagnostic Imaging*. Academic Press; 2019:73–97. doi:10.1016/B978-0-12-816086-2.00004-7
37. Verduzco-Mendoza A, Olmos-Hernández A, Bueno-Nava A, et al. Thermal imaging in biomedical research: a non-invasive technology for animal models. *Front Vet Sci*. 2025;12:1544112. PMID: 40066193; PMCID: PMC11892110. doi:10.3389/fvets.2025.1544112
38. Kakinuma Y, Furihata M, Akiyama T, et al. Donepezil, an acetylcholinesterase inhibitor against Alzheimer's dementia, promotes angiogenesis in an ischemic hindlimb model. *J Mol Cell Cardiol*. 2010;48(4):680–693. PMID: 19962381. doi:10.1016/j.yjmcc.2009.11.010
39. Sugano M, Tsuchida K, Makino N. Intramuscular gene transfer of soluble tumor necrosis factor-alpha receptor 1 activates vascular endothelial growth factor receptor and accelerates angiogenesis in a rat model of hindlimb ischemia. *Circulation*. 2004;109(6):797–802. PMID: 14970118. doi:10.1161/01.CIR.0000112579.61522.67
40. Wang L, Chen Z, Li Y, Yang J, Li Y. Optical coherence tomography angiography for noninvasive evaluation of angiogenesis in a limb ischemia mouse model. *Sci Rep*. 2019;9(1):5980. PMID: 30979948; PMCID: PMC6461622. doi:10.1038/s41598-019-42520-3
41. Kim DJ, Hahn HM, Youn YN, Lee JS, Lee IJ, Lim SH. Adipose derived stromal vascular fraction and mesenchymal stem cells improve angiogenesis in a rat hindlimb ischaemia model. *Eur J Vasc Endovasc Surg*. 2024;67(5):828–837. PMID: 37995961. doi:10.1016/j.ejvs.2023.11.036
42. Lee JJ, Arpino JM, Yin H, et al. Systematic interrogation of angiogenesis in the ischemic mouse hind limb: vulnerabilities and quality assurance. *Arterioscler Thromb Vasc Biol*. 2020;40(10):2454–2467. PMID: 32787524; PMCID: PMC7505144. doi:10.1161/ATVBAHA.120.315028
43. Holfeld J, Tepeköylü C, Blunder S, et al. Low energy shock wave therapy induces angiogenesis in acute hind-limb ischemia via VEGF receptor 2 phosphorylation. *PLoS One*. 2014;9(8):e103982. PMID: 25093816; PMCID: PMC4122398. doi:10.1371/journal.pone.0103982
44. Yan J, Tie G, Park B, Yan Y, Nowicki PT, Messina LM. Recovery from hind limb ischemia is less effective in type 2 than in type 1 diabetic mice: roles of endothelial nitric oxide synthase and endothelial progenitor cells. *J Vasc Surg*. 2009;50(6):1412–1422. PMID: 19837544; PMCID: PMC2797079. doi:10.1016/j.jvs.2009.08.007
45. Cen Y, Liu J, Qin Y, et al. Denervation in femoral artery-ligated hindlimbs diminishes ischemic recovery primarily via impaired arteriogenesis. *PLoS One*. 2016;11(5):e0154941. PMID: 27175510; PMCID: PMC4866779. doi:10.1371/journal.pone.0154941
46. Duscha BD, Kraus WE, Jones WS, et al. Skeletal muscle capillary density is related to anaerobic threshold and claudication in peripheral artery disease. *Vasc Med*. 2020;25(5):411–418. PMID: 32841100; PMCID: PMC8297535. doi:10.1177/1358863X20945794
47. Robbins JL, Jones WS, Duscha BD, et al. Relationship between leg muscle capillary density and peak hyperemic blood flow with endurance capacity in peripheral artery disease. *J Appl Physiol*. 2011;111(1):81–86. PMID: 21512146; PMCID: PMC3137528. doi:10.1152/japplphysiol.00141.2011
48. Askew CD, Green S, Walker PJ, et al. Skeletal muscle phenotype is associated with exercise tolerance in patients with peripheral arterial disease. *J Vasc Surg*. 2005;41(5):802–807. PMID: 15886664. doi:10.1016/j.jvs.2005.01.037
49. McGuigan MR, Bronks R, newton RU, et al. Muscle fiber characteristics in patients with peripheral arterial disease. *Med Sci Sports Exerc*. 2001;33(12):2016–2021. PMID: 11740293. doi:10.1097/00005768-200112000-00007

50. Kosmac K, Gonzalez-Freire M, McDermott MM, et al. Correlations of calf muscle macrophage content with muscle properties and walking performance in peripheral artery disease. *J Am Heart Assoc*. 2020;9(10):e015929. PMID: 32390569; PMCID: PMC7660852. doi:10.1161/JAHA.118.015929
51. Beaulieu RJ, Grimm JC, Hassoun HT. Ischemia - Reperfusion. In: Sidawy AN, Perler BA, editors. *Rutherford's Vascular Surgery and Endovascular Therapy*. 9th ed. Philadelphia: Elsevier; 2019:376.
52. Lejay A, Meyer A, Schlagowskia AI, et al. Mitochondria: mitochondrial participation in ischemia–reperfusion injury in skeletal muscle. *Int J Biochem Cell Biol*. 2014;50:101–105.
53. Paradis S, Charles AL, Meyer A, et al. Chronology of mitochondrial and cellular events during skeletal muscle ischemia-reperfusion. *Am J Physiol Cell Physiol*. 2016;310:C968–C982. doi:10.1152/ajpcell.00356.2015
54. White SH, McDermott MM, Sufit RL, et al. Walking performance is positively correlated to calf muscle fiber size in peripheral artery disease subjects, but fibers show aberrant mitophagy: an observational study. *J Transl Med*. 2016;14(1):284. Erratum in: J Transl Med. 2017 Feb 23;15(1):45. doi: 10.1186/s12967-017-1127-6. PMID: 27687713; PMCID: PMC5043620. doi:10.1186/s12967-016-1030-6
55. Vignaud A, Hourde C, Medja F, Agbulut O, Butler-Browne G, Ferry A. Impaired skeletal muscle repair after ischemia-reperfusion injury in mice. *J Biomed Biotechnol*. 2010;2010:724914. PMID: 20467471; PMCID: PMC2866363. doi:10.1155/2010/724914
56. Zettervall SL, Wang XL, Monk S, Lin T, Cai Y, Guzman RJ. Recovery of limb perfusion and function after hindlimb ischemia is impaired by arterial calcification. *Physiol Rep*. 2021;9(16):e15008. PMID: 34405571; PMCID: PMC8371346. doi:10.14814/phy2.15008
57. Foussard N, Bourguignon C, Grouthier V, et al. ICAM1 blockade improves ischemic muscle reperfusion in diabetic mice. *Cardiovasc Diabetol*. 2025;24(1):20. PMID: 39827135; PMCID: PMC11742775. doi:10.1186/s12933-025-02573-3
58. Ryan TE, Schmidt CA, Alleman RJ, et al. Mitochondrial therapy improves limb perfusion and myopathy following hindlimb ischemia. *J Mol Cell Cardiol*. 2016;97:191–196. PMID: 27262673; PMCID: PMC5002368. doi:10.1016/j.yjmcc.2016.05.015
59. Wang T, Zhou YT, Chen XN, Zhu AX. Putative role of ischemic postconditioning in a rat model of limb ischemia and reperfusion: involvement of hypoxia-inducible factor-1a expression. *Braz J Med Biol Res*. 2014;47(9):738–745. doi:10.1590/1414-431X20142910
60. Pfaff MJ, Mukhopadhyay S, Hoofnagle M, Chabasse C, Sarkar R. Tumor suppressor protein p53 negatively regulates ischemia-induced angiogenesis and arteriogenesis. *J Vasc Surg*. 2018;68(6S):222S–233S.e1. PMID: 30126780; PMCID: PMC10981785. doi:10.1016/j.jvs.2018.02.055
61. Baron-Menguy C, Bocquet A, Richard A, et al. Sildenafil-induced revascularization of rat hindlimb involves arteriogenesis through PI3K/AKT and eNOS activation. *Int J Mol Sci*. 2022;23(10):5542. PMID: 35628350; PMCID: PMC9143320. doi:10.3390/ijms23105542
62. Hedhli J, Kim M, Knox HJ, et al. Imaging the landmarks of vascular recovery. *Theranostics*. 2020;10(4):1733–1745. PMID: 32042333; PMCID: PMC6993245. doi:10.7150/thno.36022
63. Ali AMEA, Ahmed AS, El-Yasergy DF, et al. Therapeutic potential of mesenchymal stem cells for peripheral artery disease in a rat model of hindlimb ischemia. *Iran J Basic Med Sci*. 2021;24(6):805–814. PMID: 34630958; PMCID: PMC8487602. doi:10.22038/ijbms.2021.55861.12491
64. Schmeisser K, Parker JA. Pleiotropic effects of mTOR and autophagy during development and aging. *Front Cell Dev Biol*. 2019;7:192.
65. Mihaylova MM, Shaw RJ. The AMPK signalling pathway coordinates cell growth, autophagy and metabolism. *Nat Cell Biol*. 2011;13(9):1016–1023. PMID: 21892142; PMCID: PMC3249400. doi:10.1038/ncb2329
66. Xu MJ, Song P, Shirwany N, et al. Impaired expression of uncoupling protein 2 causes defective postischemic angiogenesis in mice deficient in AMP-activated protein kinase α subunits. *Arterioscler Thromb Vasc Biol*. 2011;31(8):1757–1765. PMID: 21597006; PMCID: PMC3158995. doi:10.1161/ATVBAHA.111.227991
67. Scalabrin M, Engman V, Maccannell A, et al. Temporal analysis of skeletal muscle remodeling post hindlimb ischemia reveals intricate autophagy regulation. *Am J Physiol Cell Physiol*. 2022;323(6):C1601–C1610. PMID: 36252128; PMCID: PMC9722248. doi:10.1152/ajpcell.00174.2022
68. Mathiassen SG, DeZio D, Cecconi F. Autophagy and the cell cycle: a complex landscape. *Front Oncol*. 2017;7:51. doi:10.3389/fonc.2017.00051
69. Hewitt G, Korolchuk VIR. Reuse, recycle: the expanding role of autophagy in genome maintenance. *Trends Cell Biol*. 2017;27(5):340–351. doi:10.1016/j.tcb.2016.11.011
70. Jeong IH, Bae WY, Choi JS, Jeong JW. Ischemia induces autophagy of endothelial cells and stimulates angiogenic effects in a hindlimb ischemia mouse model. *Cell Death Dis*. 2020;11:624. doi:10.1038/s41419-020-02849-4
71. Pugsley HR. Assessing autophagic flux by measuring LC3, p62, and LAMP1 co-localization using multispectral imaging flow cytometry. *J Vis Exp*. 2017;125:55637.
72. Neel BA, Lin Y, Pessin JE. Skeletal muscle autophagy: a new metabolic regulator. *Trends Endocrinol Metab*. 2013;24(12):635–643. doi:10.1016/j.tem.2013.09.004
73. He L, Zhang J, Zhao J, et al. Autophagy: the last defense against cellular nutritional stress. *Adv Nutr*. 2018;9:493–504. doi:10.1093/advances/nmy011
74. Albadawi H, Oklu R, Milner JD, et al. Effect of limb demand ischemia on autophagy and morphology in mice. *J Surg Res*. 2015;198(2):515–524. PMID: 25959834; PMCID: PMC4560984. doi:10.1016/j.jss.2015.04.008
75. McClung JM, McCord TJ, Ryan TE, et al. BAG3 (Bcl-2-Associated Athanogene-3) coding variant in mice determines susceptibility to ischemic limb muscle myopathy by directing autophagy. *Circulation*. 2017;136(3):281–296. PMID: 28442482; PMCID: PMC5537727. doi:10.1161/CIRCULATIONAHA.116.024873
76. Liu C, Peng M, Zheng L, et al. Enhanced autophagy alleviates injury during hindlimb ischemia/reperfusion in mice. *Exp Ther Med*. 2019;18(3):1669–1676. PMID: 31410124; PMCID: PMC6676216. doi:10.3892/etm.2019.7743
77. Martinelli O, Peruzzi M, Bartimoccia S, et al. Natural activators of autophagy increase maximal walking distance and reduce oxidative stress in patients with peripheral artery disease: a pilot study. *Antioxidants*. 2022;11(9):1836. PMID: 36139910; PMCID: PMC9495993. doi:10.3390/antiox11091836
78. Pass CG, Palzkill V, Tan J, et al. Single-Nuclei RNA-sequencing of the gastrocnemius muscle in peripheral artery disease. *Circ Res*. 2023;133(10):791–809. PMID: 37823262; PMCID: PMC10599805. doi:10.1161/CIRCRESAHA.123.323161
79. Goto T, Fukuyama N, Aki A, et al. Search for appropriate experimental methods to create stable hind-limb ischemia in mouse. *Tokai J Exp Clin Med*. 2006;31(3):128–132.
80. Dragneva G, Korpisalo P, Herttuala SY. Promoting blood vessel growth in ischemic diseases: challenges in translating preclinical potential into clinical success. *Dis Models Mech*. 2013;312–322. doi:10.1242/dmm.010413
81. Aref Z, de Vries MR, Quax PHA. Variations in surgical procedures for inducing hind limb ischemia in mice and the impact of these variations on neovascularization assessment. *Int J Mol Sci*. 2019;20:3704. doi:10.3390/ijms20153704